

Compound Barker-Coded Excitation for Increased Signal-to-Noise Ratio and Penetration Depth in Transcranial Ultrasound Imaging

Emelina Vienneau and Brett Byram
Department of Biomedical Engineering
Vanderbilt University
Nashville, TN, USA
emelina.p.vienneau@vanderbilt.edu

Abstract—Clinical translation of transcranial ultrasound imaging has been unsuccessful due to poor image quality. One cause is insufficient signal-to-noise ratio (SNR) due to poor acoustic penetration through the skull. Coded excitation can be used to increase SNR within FDA safety limits and without contrast agents. This work encompasses a method to design long binary coded pulses along with a pulse compression technique to completely suppress range lobes, thereby recovering axial resolution and improving SNR by as much as a factor of $10\log_{10}(\text{code length})$. This optimized coded excitation framework was shown to be effective in transcranial imaging of five healthy adult subjects.

I. INTRODUCTION

Robust transcranial ultrasound imaging is difficult due to poor image quality, a barrier that still impedes clinical translation. The high acoustic impedance mismatch between the skull and surrounding tissue greatly reduces acoustic penetration and therefore the signal-to-noise ratio (SNR). Microbubble contrast agents are one approach to solving this problem, but reliance on contrast agents increases the scan time, complexity, and invasiveness of the procedure, ultimately making them impractical for many applications. An alternative solution to this problem is coded excitation.

The goal of coded excitation is to increase the time-bandwidth product of the transmitted pulse by modulating it such that the backscattered echoes can be demodulated, thereby recovering the original pulse width but with a higher signal power. Design of a coded excitation framework in medical ultrasound must take several factors into consideration, including the SNR gain, the range lobe levels, the complexity of implementation, and robustness to motion and frequency-dependent attenuation [1]. Successful coded excitation schemes in medical ultrasound utilize frequency modulation and/or phase modulation. Frequency modulated waveforms such as linear instantaneous frequency chirp signals are a popular approach that often yields great benefits to SNR since chirps can incorporate the full bandwidth of the transducer and can be designed to be very long, provided that they are not so long that the pulser suffers from voltage droop or the pulse length becomes larger than the depth of focus [1], [2]. However, in order to suppress range lobes that arise from

pulse compression, chirps are best implemented with a multi-state pulser capable of significant amplitude shaping rather than the tri-state pulsers that are available in most systems. While pseudo-chirps can be implemented with tri-state pulsers, the range lobes become much higher than desired [2].

In contrast, phase modulation is far simpler to implement and does not require complex hardware, making it a more practical coded excitation approach for many ultrasound applications [2]. Phase modulation is achieved by convolving a base pulse with a binary sequence of +1s and -1s that represent 0° and 180° phase shifts. Phase modulation can either be implemented with one transmit such as with a Barker code or a m-sequence or it can be implemented with multiple transmits such as with complimentary Golay codes. While complimentary sequences can theoretically yield perfect pulse compression, any target motion between frames hinders pulse compression, resulting in a smaller gain in SNR and the appearance of range lobes that degrade contrast and obscure nearby signals of interest. Single transmit phase encoding approaches are far more robust to target motion and can yield sizeable improvements in SNR with long enough codes [1]–[3]. Barker codes are used most often for single transmit phase modulation since m-sequences and other sub-optimal binary sequences lead to much higher range lobes when compressed with a matched filter [1]. However, the longest known Barker code is only 13 bits long, so the maximum achievable SNR gain is only $10\log_{10}(13) = 11$ dB while the range lobes are $20\log_{10}(13) = 22.3$ dB below the maximum, an unacceptable loss in dynamic range for a modest increase in SNR [1], [4].

In this work, we present an alternative coded excitation framework based on compound Barker codes and inverse filtering that optimizes for SNR gain, hardware complexity, range lobe levels, and robustness to motion. Although the use of compound Barker codes and inverse filtering have both been reported separately in the literature [2], [3], [5]–[7], this work is the first to the authors' knowledge to combine these two techniques for coded excitation in medical ultrasound. The goal of this work is to demonstrate the feasibility and efficacy of this coded excitation framework for increasing the SNR of *in vivo* transcranial ultrasound imaging.

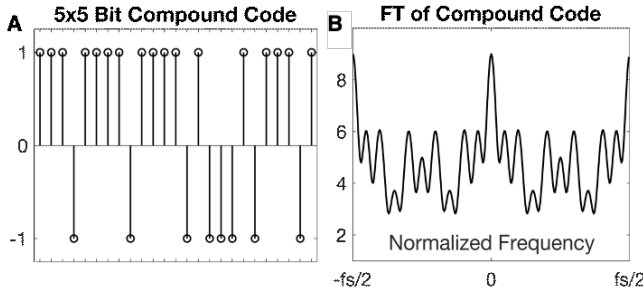


Fig. 1. 5x5 (25 bit) compound Barker code and its Fourier Transform, which has no zeros.

II. METHODS

A. Formation of Compound Barker-Coded Waveforms

Barker codes longer than 2 bits have the property that they have no zeros in their spectrum, so stable pseudo-inverse filters can be constructed [3]. Furthermore, Barker codes can be combined via the Kronecker product to create longer binary sequences referred to as compound Barker codes that still have full spectral support as shown in Fig. 1. This approach allows for the creation of binary sequences of almost any length that can be compressed very well, offering the opportunity to achieve dramatic improvements in SNR without complex hardware or any degradation to image quality.

To create the coded excitation waveform that is transmitted by the transducer, this compound code must be upsampled and convolved with a chip pulse such as a single cycle sine wave that defines the axial resolution and fits within the bandwidth of the transducer. For a tri-state pulser such as the Verasonics, this is as simple as convolving the compound code with the waveform defined by the series of 1s, 0s, and -1s corresponding to positive rail voltage, ground, and negative rail voltage, respectively, that makes up the desired base pulse as shown in Fig. 2.

B. Construction of the Decoding Filter

In place of matched or mismatched filtering, inverse filtering can be used instead for code compression since these compound Barker codes have full spectral support. This is in contrast to frequency modulation approaches, which must rely on mismatched filtering to suppress range lobes. Instead of maximizing the signal energy, inverse filtering minimizes the error between the desired spectrum and the calculated spectrum in the least squares sense, so the range lobes are theoretically suppressed completely [3]. In practice, the range lobes are beyond -80 dB, far below the dynamic range required by most clinical ultrasound applications. Further, the loss in SNR gain from inverse filtering instead of matched filtering is generally less than 1 dB and often as low as about 0.2 dB, an acceptable trade-off considering the large gains in range lobe reduction [8], [9].

The decoding filter is created by constructing an L -tap FIR approximation to the inverse spectrum of the code. The

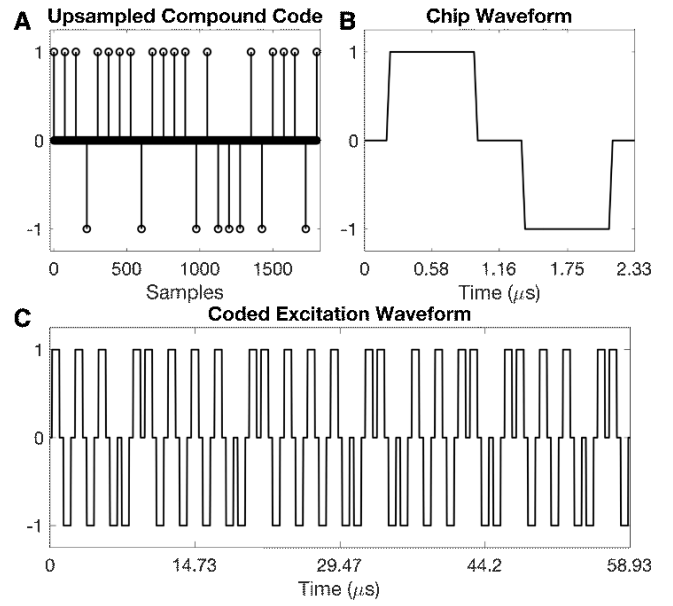


Fig. 2. Creation of coded excitation waveform. (A) Upsampled compound Barker code. (B) Tri-state chip waveform corresponding to a 2.72 MHz sine wave. (C) Convolution of upsampled code and chip pulse create the coded excitation waveform.

approach and notation of Gran *et al.* was followed for this procedure [3]. This approach amounts to taking the first L samples of the inverse discrete Fourier transform of the desired inverse spectrum. A brief overview is provided here. To determine the desired inverse spectrum, the discrete Fourier transform of the compound code needs to be calculated according to Eqn. (1).

$$C(f) = \sum_{n=0}^{N-1} c(n) e^{-2\pi j(f/f_s)n}, \quad -\frac{f_s}{2} \leq f < \frac{f_s}{2} \quad (1)$$

The desired inverse spectrum can then be calculated from the inversion of Eqn. (1), which is allowed because the compound codes have no zeroes in the Fourier domain. The phase-corrected inverse spectrum is given by Eqn. (2).

$$D(f) = \frac{e^{-j\pi(f/f_s)L}}{C(f)e^{j\pi(f/f_s)N}}, \quad -\frac{f_s}{2} \leq f < \frac{f_s}{2} \quad (2)$$

This inverse spectrum is evaluated on M points within the range of $-\frac{f_s}{2} \leq f < \frac{f_s}{2}$, where $M > L > N$. This can be achieved with Fourier matrices. To evaluate Eqn. (1), the $M \times N$ Fourier matrix is multiplied by the N length compound code. Equation (2) can then be computed. To compute the first L FIR filter coefficients, Eqn. (2) must be multiplied by the $M \times L$ Fourier matrix. This inverse filter is given by Eqn. (3),

$$\hat{h}(l) = \frac{1}{M} \sum_{m=0}^{M-1} D(f_m) e^{2\pi j(lm/M)}, \quad (3)$$

where l ranges from 0 to $L-1$ and m ranges from 0 to $M-1$. To construct the final decoding filter for the coded excitation waveform, the convolution with the chip pulse must be taken into account. The inverse filter from Eqn. (3) is

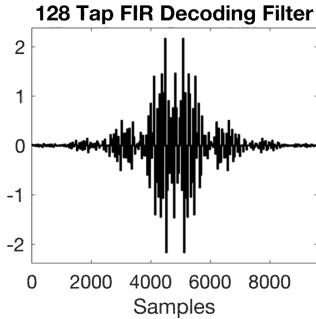


Fig. 3. Decoding filter used for pulse compression.

therefore upsampled and convolved with the time-reversed chip waveform according to Eqn. (4),

$$g(n) = \sum_{l=0}^{L-1} h(l)p(-n + lTf_s), \quad (4)$$

where T is the time duration between bits (often the length of the chip pulse), p is the chip, and f_s is the sampling frequency of the ultrasound system. A 128 tap decoding filter is shown in Fig. 3. In effect, the decoding filter serves as a matched filter for the chip pulse and an inverse filter for the compound Barker code, leading to complete code compression. It should be noted that the longer the compound code, the larger L needs to be to achieve good compression.

C. Image Acquisition and Processing

In vivo transcranial imaging of five healthy adult subjects as well as imaging of a CIRS phantom was performed with a 64-element P4-2v phased array (0.3 mm pitch) operating at 2.72 MHz and a Verasonics Vantage 128 ultrasound scanner. Twenty frames and 128 beams were acquired with a frame rate of 18 Hz, an imaging depth of 16 cm, and a transmit focus of 8 cm. For the transcranial *in vivo* imaging, the transducer was placed over the subject's temporal bone at the acoustic window. The probe was hand-held and angled to capture the transverse plane. The probe was placed in a holder to capture the phantom data. The decoding filter derived in Section II-B and shown in Fig. 3 ($M = 300$) was applied on the channel data, but only minimal differences were observed when it was applied on the beamsummed RF data. In practice, decoding can usually be performed on the beamsummed data unless the imaging depth is very shallow or the image quality of the near-field needs to be preserved. Dynamic receive beamforming was applied to the channel data after decoding. The transmit sequences tested were a single cycle pulse (baseline uncoded approach) as in Fig. 2B, a 5 bit Barker code, a 13 bit Barker code, and a 5x5 (25 bit) compound Barker code as in Fig. 2C. The chip waveform for each of the coded approaches was the same single cycle tri-state pulse as in Fig. 2B. The derated ISPPA was matched for all transmit waveforms and acoustic output was measured with a hydrophone and deemed safe according to the FDA limits.

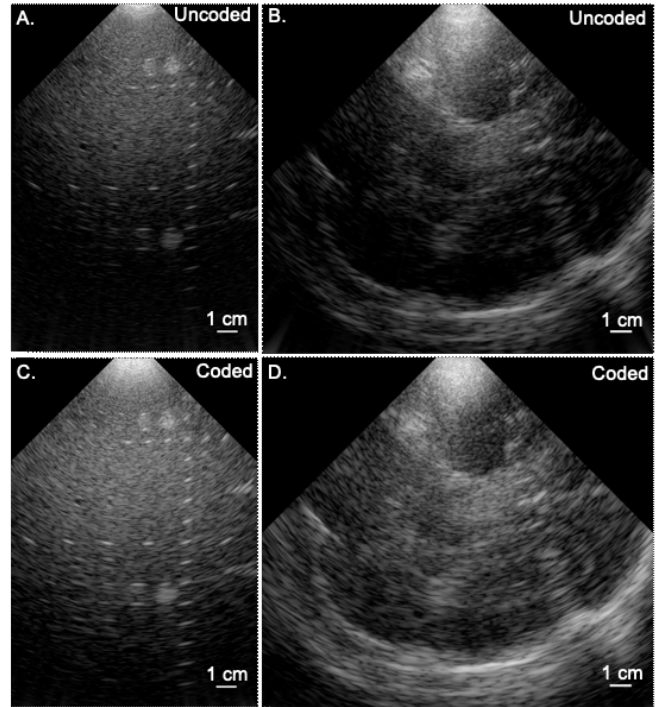


Fig. 4. Qualitative improvement of applying coded excitation. CIRS phantom (A and C) and *in vivo* transcranial (B and D) images of uncoded and coded excitation approaches. Coded excitation approaches shown here used a 25 bit compound Barker code. Note increased signal in the coded images, particularly at depth. Images all shown on 70 dB dynamic range.

D. SNR Gain Measurements

To measure the SNR gain due to coded excitation in the phantom and *in vivo* data, SNR was calculated according to Eqn. (5),

$$\text{SNR} = 10\log_{10} \left(\frac{\rho}{1 - \rho} \right), \quad (5)$$

where ρ represents the normalized cross-correlation (NCC) estimate.

III. RESULTS

Qualitative improvements in SNR using coded excitation in a CIRS phantom and *in vivo* transcranial imaging in a healthy adult subject can be seen in Fig. 4. The coded excitation approach shown here is the 25 bit compound Barker code as in Fig. 2C. Note the improvements in signal strength especially at deeper depths. Importantly, the improvements in the transcranial image are comparable to those in the phantom image. This demonstrates that the coded excitation framework presented herein is efficacious even in a challenging *in vivo* scenario with significant frequency-dependent attenuation.

Numerical results are presented in Table I, which shows the SNR gain from coded excitation approaches vs. the uncoded approach as a function of code length. Gains are presented in dB and errors represent standard deviation, with $n=2$ for the phantom cases and $n=34$ for the *in vivo* cases. Due to the low frame rate and unmitigated out-of-plane subject/sonographer

TABLE I
SNR VS. CODE LENGTH

Code Length	Phantom (NCC)	In vivo (NCC)	In vivo (Amplitude)	Theor. Gain
5	6.42 \pm 0.06	2.96 \pm 0.43	4.60 \pm 1.33	7 dB
13	10.09 \pm 0.32	3.03 \pm 0.65	11.55 \pm 3.87	11 dB
25	11.32 \pm 0.56	3.14 \pm 0.51	12.64 \pm 2.23	14 dB

motion in the *in vivo* data, the SNR gain measured with Eqn. (5) greatly underestimated the observed qualitative benefits which matched those of the phantom. In order to estimate the gain in signal strength due to coded excitation in the *in vivo* images, the amplitudes in bright, stable ROIs in the skull were also compared. These values are shown in the column labeled “Amplitude”, as opposed to NCC, which refers to the normalized cross-correlation approach described by Eqn. (5). The SNR gains in the phantom and the amplitude gains in transcranial imaging approach the theoretical gains shown in the rightmost column of Table I. Additional experimental studies should be performed in the future with faster frame rates in order to more accurately estimate the SNR gain *in vivo*. Further studies will also explore much longer compound codes which have the potential to improve SNR gains even further. However, the results to date demonstrate that large SNR gains can be realized *in vivo* with the proposed coded excitation framework.

IV. CONCLUSION

In summary, we showed that compound Barker codes coupled with inverse filtering for decoding serve as an effective coded excitation framework for improving SNR of ultrasound imaging in challenging scenarios such as transcranial imaging of adult subjects. We demonstrated a 12 dB SNR improvement in *in vivo* transcranial imaging which approaches theoretical expectations.

ACKNOWLEDGMENT

The authors would like to acknowledge the staff at Vanderbilt University’s Advanced Computing Center for Research and Education (ACCRE) for their continued support. This work has been supported by the award T32EB021937 from the National Institutes of Health as well as the award IIS-1750994 from the National Science Foundation.

REFERENCES

- [1] T. Misaridis and J. A. Jensen, “Use of modulated excitation signals in medical ultrasound. Part I: Basic Concepts and Expected Benefits,” *IEEE Transactions on Ultrasonics, Ferroelectrics, and Frequency Control*, vol. 52, no. 2, pp. 177–191, 2005.
- [2] R. Y. Chiao and X. Hao, “Coded Excitation for Diagnostic Ultrasound: A System Developer’s Perspective,” *IEEE Transactions on Ultrasonics, Ferroelectrics and Frequency Control*, vol. 52, no. 2, pp. 160–170, 2005.
- [3] F. Gran, J. Udesen, M. B. Nielsen, and J. A. Jensen, “Coded ultrasound for blood flow estimation using subband processing,” *IEEE Transactions on Ultrasonics, Ferroelectrics, and Frequency Control*, vol. 55, no. 10, pp. 2211–2220, 2008.
- [4] R. H. Barker, *Communication Theory*. London: Butterworth, 1953, ch. Group Synchronizing of Binary Digital Sequences, pp. 273–287.
- [5] B. Kiranmai and P. Rajesh Kumar, “Performance Evaluation of Compound Barker Codes using Cascaded Mismatched Filter Technique,” *International Journal of Computer Applications*, vol. 121, no. 19, pp. 31–34, 2015.
- [6] J. Udesen, F. Gran, K. L. Hansen, J. A. Jensen, C. Thomsen, and M. B. Nielsen, “High frame-rate blood vector velocity imaging using plane waves: Simulations and preliminary experiments,” *IEEE Transactions on Ultrasonics, Ferroelectrics, and Frequency Control*, vol. 55, no. 8, pp. 1729–1743, 2008.
- [7] H. Zhao, L. Y. L. Mo, and S. Gao, “Barker-coded ultrasound color flow imaging: Theoretical and practical design considerations,” *IEEE Transactions on Ultrasonics, Ferroelectrics, and Frequency Control*, vol. 54, no. 2, pp. 319–330, 2007.
- [8] R. C. Daniels and V. Gregers-Hansen, “Code inverse filtering for complete sidelobe removal in binary phase coded pulse compression systems,” *IEEE National Radar Conference - Proceedings*, vol. 2005-Janua, no. January, pp. 256–261, 2005.
- [9] Y. Wang, K. Metzger, D. N. Stephens, G. Williams, S. Brownlie, and M. O’Donnell, “Coded Excitation with Spectrum Inversion (CEXI) for Ultrasound Array Imaging,” *IEEE Transactions on Ultrasonics, Ferroelectrics, and Frequency Control*, vol. 50, no. 7, pp. 805–823, 2003.